

Flexible EMI shielding materials derived by melt blending PVDF and ionic liquid modified MWNTs

This content has been downloaded from IOPscience. Please scroll down to see the full text.

View [the table of contents for this issue](#), or go to the [journal homepage](#) for more

Download details:

IP Address: 128.112.200.107

This content was downloaded on 11/11/2014 at 07:23

Please note that [terms and conditions apply](#).

## Flexible EMI shielding materials derived by melt blending PVDF and ionic liquid modified MWNTs

Maya Sharma<sup>1</sup>, Sukanya Sharma<sup>2</sup>, Jiji Abraham<sup>3</sup>, Sabu Thomas<sup>3</sup>,  
Giridhar Madras<sup>1</sup> and Suryasarathi Bose<sup>2</sup>

<sup>1</sup> Center for Nano Science and Engineering, Indian Institute of Science, Bangalore-560012, India

<sup>2</sup> Department of Materials Engineering, Indian Institute of Science, Bangalore-560012, India

<sup>3</sup> International and Interuniversity Centre for Nanoscience and Nanotechnology, Mahatma Gandhi University, Kottayam, Kerala 686560, India

E-mail: [sbose@materials.iisc.ernet.in](mailto:sbose@materials.iisc.ernet.in)

Received 5 May 2014, revised 4 June 2014

Accepted for publication 16 June 2014

Published 2 July 2014

*Materials Research Express* 1 (2014) 035003

doi:[10.1088/2053-1591/1/3/035003](https://doi.org/10.1088/2053-1591/1/3/035003)

### Abstract

Nano composites of PVDF with ionic liquid [EMIM][TF<sub>2</sub>N] (IL) modified MWNTs were prepared by melt blending to design materials for EMI shielding applications. MWNTs and IL were mixed in two different ratios (1:1 and 1:5) to facilitate better dispersion of MWNTs in PVDF. It was observed that non-covalent interactions between IL and PVDF resulted in a better dispersion of CNTs and was consistent with increasing concentration of IL. Interestingly, IL modified MWNTs induced the formation of  $\gamma$ -phase crystals in PVDF, which was further confirmed by XRD, FTIR and DSC. Melt rheological measurements and DSC analysis revealed the plasticization effect of IL in PVDF composites further manifesting in a decrease in the storage modulus and the glass transition temperature. This phenomenal effect presumably led to better dispersion of IL modified MWNTs in PVDF further resulting in a significant improvement in electrical conductivity and structural properties. More interestingly, the elongational properties in the composites improved with IL modified MWNTs in striking contrast to MWNT filled PVDF composites. The ac conductivity of the composites reached about  $10^{-3} \text{ S cm}^{-1}$  with the addition of 2 wt% IL modified MWNTs (1:1). This further led to a high electro-magnetic interference (EMI) shielding effectiveness of about 20 dB at 2 wt% IL modified MWNTs. Such materials can further be explored for flexible, lightweight EMI shielding materials for a wide range of operating frequency.

Keywords: PVDF, MWNT, ionic liquid, EMI shielding

## 1. Introduction

Nano-composites are receiving an increasing surge of interest owing to their superior physical and chemical properties and are currently being explored for a wide range of applications. In this era of rapidly advancing technology, the operating frequency of most of the devices alarmingly increases, leading to a new kind of problem called EM (electromagnetic) pollution. This can, besides interfering with the surrounding devices, pose serious health risks to living beings in the vicinity of the appliances [1]. Thus, these instruments need to be equipped with EMI (electromagnetic interference) shielding materials. The materials are designed such that they act as a shield to the radiation being emitted that can interfere with surrounding gadgets to cause mutual disturbances and glitches in their continuous functioning [2]. Most appliances used commercially or in military applications operate in the frequency range of 8.4–12.4 GHz; more commonly known as the X-band. The applications of these shields also depend on the mechanism employed by it while shielding. The two well-known mechanisms are absorption and reflection of the incident radiation. Reflection is caused by the presence of mobile charge carriers and absorption is due to electric and magnetic dipoles. They interact with the electromagnetic field present in the radiation and render them harmless [3].

Polymer based conducting composites are lighter and have easier processability and can be used as EMI shielding materials [4]. In this context, poly vinylidene fluoride (PVDF), a semi crystalline polymer, is known to possess high dielectric constant, chemical resistance and thermal stability coupled with good mechanical properties. PVDF is widely being used as a piezoelectric material [5, 6] with a net dipole moment [7]. These characteristics make PVDF a suitable matrix for EMI shielding applications. PVDF by itself is an insulating polymer and is thus transparent to the EM waves. This property can be significantly altered by incorporating conducting particles [8–11].

Carbon nanotubes (CNTs) are formed by the rolling of exfoliated graphene sheets. They have excellent physical [12], electrical [13] and thermal [14] properties which make them the ideal choice for polymer based nanocomposites. Another striking feature of these particles which make them widely used as fillers for conducting and EMI shielding applications is that they possess good EM properties [15].

Shielding by reflection would require charge carriers which can make the sample electrically conducting [3]. Conductivity would require a good network formation of the filler material [16]. A good dispersion of CNTs would ensure good conductivity and mechanical properties to design flexible EMI shielding materials which can find use in commercial applications. Dispersion of CNTs has always posed a problem as CNTs tend to agglomerate owing to the strong  $\pi$ - $\pi$  interaction. One way to disperse them is to covalently graft functional moieties on the surface [17]. However, this route largely disrupts the  $\pi$  electron cloud on CNTs. Alternatively, non-covalent modification does not disrupt the surface of the CNTs, and their mechanical and electrical properties remain intact. An emerging way of making the CNTs interact with ionic liquids is via a cation- $\pi$  interaction [18]. Ionic liquids are salts in their liquid phase at room temperature and have virtually no vapor pressure [19]. Their applications currently comprise separation technology, homogenous catalysis, templates for zeolites etc. They possess good thermal stability, non-flammability and high conductivity. They have been introduced as a substitution for organic solvents and offer a high temperature range with improved safety [19]. It is well established that CNTs with ionic liquids lead to the formation of

physical gels [20]. Ionic liquids improve the dispersion of CNTs in the matrix and also lead to an improvement in the piezo electric properties of the composites [17, 18, 21].

Our current focus is to improve the electrical conductivity and EMI shielding properties of the PVDF/MWNT based nanocomposites while retaining the mechanical aspects of the pristine polymer (PVDF). In the recent past, various groups have reported the EMI values of various polymeric systems with different fillers. Lee *et al* reported a shield effectiveness (SE) of close to 10 dB with 10% carbon fibers loaded in the PVDF samples [13]. An SE of 20 dB was reported with 35% carbon black fillers in EPDM and similar loading and SE with carbon black for SBR matrix [8]. Joseph *et al* reported an SE of 26 dB with very high filler loadings in PVDF (20 vol% nano-BaTiO<sub>3</sub> and 10 vol% of Ag) [12]. Eswaraiah *et al* reported an SE of 18–20 Db with the addition of 1% MWNTs and 5% MnO<sub>2</sub> particles [22]. It is well documented that higher loadings of CNT tend to agglomerate thereby leading to detrimental effects on the structural properties of the nanocomposites. Therefore, achieving higher electrical conductivity and EMI at lower fractions of CNTs is the current challenge as this also ensures the structural integrity of the nanocomposites.

To address this challenge, MWNTs were non-covalently modified with ionic liquid, 1-ethyl 3-methylimidazolium bis (trifluoromethyl sulphonyl imide), to facilitate better dispersion of MWNTs in the PVDF matrix. The content of the IL was varied in the mixture of IL and MWNTs. Mechanical properties of the composites such as tensile strength and elongational properties were studied in the presence of ionic liquid modified CNTs. Electrical conductivity and EMI SE was assessed for MWNTs and various ratios of IL modified MWNTs. Finally, attempts have been made to correlate the morphology with properties.

## 2. Experimental

### 2.1. Materials

Kynar PVDF 740 was supplied by Arkema. CNTs were obtained from Nanocyl (grade: NC 7000) and were further processed to avoid agglomeration in the composites. Ionic liquid, 1-ethyl 3-methylimidazolium bis (trifluoromethyl sulphonyl imide), EMIMTf<sub>2</sub>N was procured from Sigma Aldrich and used as-received. CNTs were mixed with IL in two different ratios namely 1:1 and 1:5. For instance, for 1:1 ratio of CNT and ionic liquid, we mix 1 gm CNT with 1 mmol of ionic liquid (1 mmol = Molecular weight/1000). First, they were physically mixed by grinding in a mortar for 30 min. The mixture was further sonicated in ethanol for 30 min in an ultrasonic bath followed by drying at 80 °C under vacuum [23].

### 2.2. Preparation of melt-mixed samples

All composites were prepared by melt blending using HAAKE extruder CTWS at 220 °C for 20 min with a screw speed of 60 rpm. Strands obtained from melt mixing were further molded into discs and thin films by compression molding. The designations of the composites used can be found listed in table 1.

### 2.3. Characterization of CNT:IL

For analyzing IL modified CNTs, x-ray photon scattering (XPS) spectra were recorded using a Kratos Analytical instrument with Al monochromatic source (1.486 keV). Further confirmation

**Table 1.** Designations of the composites prepared.

Serial No.	Sample Name	Ratio of CNT:IL	Wt(%) of CNTs	Designation
1	Neat PVDF		0%	PVDF
2	Pristine CNT		1%	PVDF with 1% p-CNT
			2%	PVDF with 2% p-CNT
3	PVDF + CNT + IL (1:1)	(1:1)	1%	PVDF with 1 wt% IL-MWNTs (1:1)
			2%	PVDF with 2 wt% IL-MWNTs (1:1)
4	PVDF + CNT + IL (1:5)	(1:5)	1%	PVDF with 1 wt% IL-MWNTs (1:5)
			2%	PVDF with 2 wt% IL-MWNTs (1:5)

of IL was done using FTIR (Thermo Nicolet 6700) spectra using KBr pellets in the wavelength range of 400–4000  $\text{cm}^{-1}$ .

#### 2.4. Characterization of composites

To study the crystal phases, x-ray diffraction patterns were obtained using a PANalytical X'pert Pro using a Cu  $K\alpha$  radiation having a wavelength of 0.154 nm and energy of 40 keV. The  $2\theta$  values ranged from 5–50° with a scan rate of 0.04  $\text{s}^{-1}$ . The Fourier transform infrared spectroscopy (FTIR) peaks were obtained by a Perkin Elmer spectrometer GX using thin films (100  $\mu\text{m}$ ) by accumulating 32 scans ranging from 600–4000  $\text{cm}^{-1}$ , with a resolution of 0.4  $\text{cm}^{-1}$ . Thermal and crystallization properties of composites were studied using DSC. Scans were done by means of a DSC (differential scanning calorimetry, TA Q2000). In the first heating, the composites were heated to a melt miscible state (200 °C) and held for 5 min to ensure complete miscibility. Samples were then cooled to –50 °C at 10 K  $\text{min}^{-1}$  followed by second heating cycle reaching a temperature of 200 °C at 10 K  $\text{min}^{-1}$ . All the experiments were performed under a nitrogen environment.

Rheological response of the composites of PVDF-IL modified CNTs was characterized by Rheometer (DHR-3, TA Instruments) using dynamic small amplitude oscillatory shear with parallel plate geometry (25 mm in diameter and gap distance of 1 mm). Experiments were carried out at 200 °C, 100–0.01  $\text{rad s}^{-1}$ , 1% strain. To prevent the oxidation of the composites at elevated temperatures, all measurements were performed under nitrogen.

Discs of 10 mm diameter were prepared for the dielectric measurements. The composites were coated with silver paste on either side to ensure better contact and homogenous charge transfer. Dielectric measurements were carried out using an Alpha-N analyzer, Novocontrol in a broad frequency range of  $10^{-2}$ – $10^7$  Hz. The morphology and dispersion of the modified CNTs were studied using a field emission scanning electron microscope (ULTRA 55 Zeiss FESEM). The SE of the composites was calculated in the X and Ku band using an Anritsu MS4642A Vector Network Analyzer (VNA). A coupling was established between the VNA and a coax set-up (Damaskos M 07T). We carried out a two-port full SOLT calibration of the setup. A micro UTM was used to conduct tensile tests on thin polymer films using a load cell of 100 N and a strain rate of 25  $\text{mm min}^{-1}$  and the composites were tested till failure.

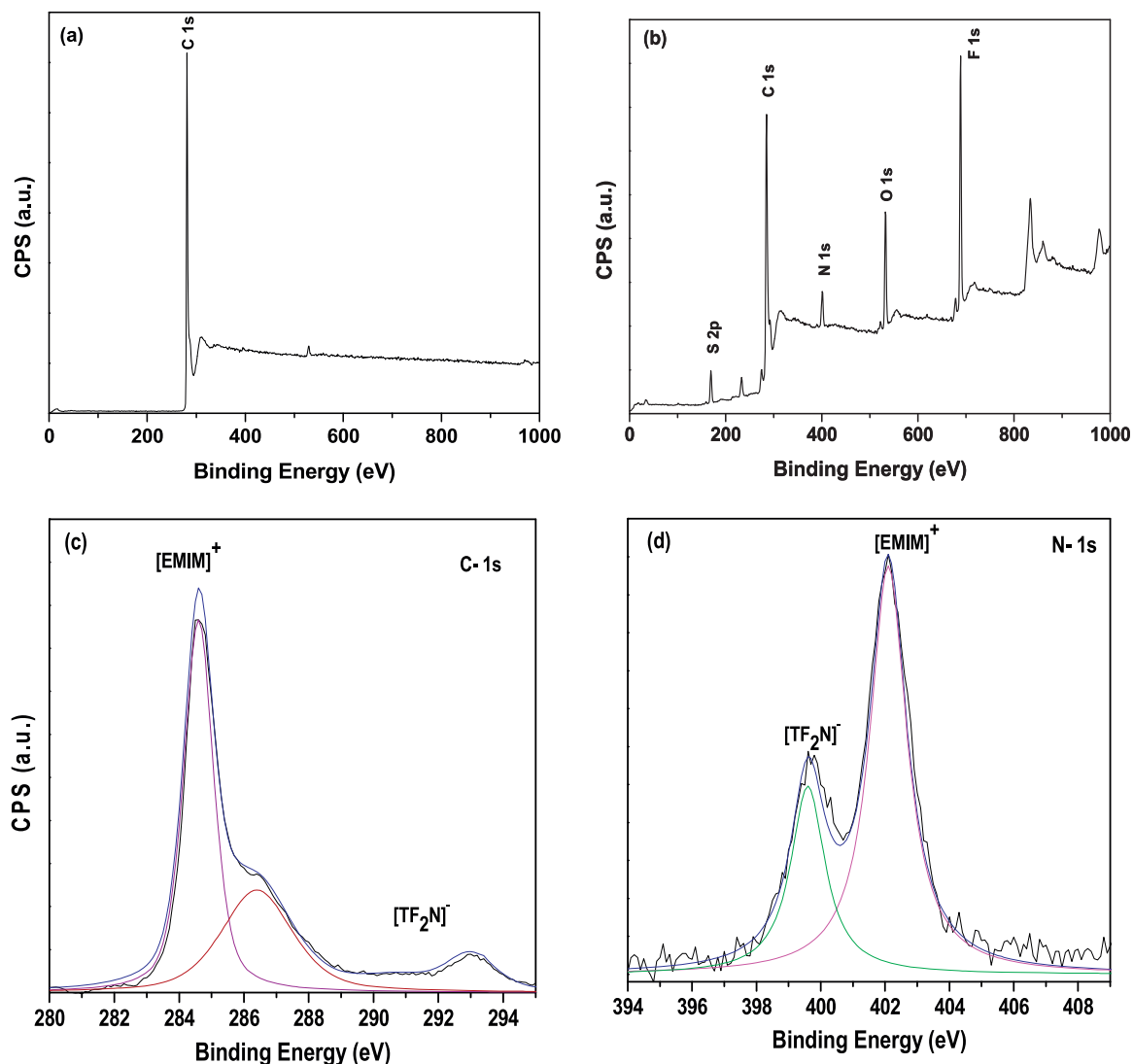


**Figure 1.** XPS spectra for p-CNT (a) and for IL modified CNTs, (b) high resolution convoluted plots for C 1s (c) and for N 1s (d).

### 3. Results and discussions

#### 3.1. Synthesis and characterization of IL modified MWNTs

MWNTs were modified with IL as described in the experimental section. Presence of IL on the surface of MWNTs is confirmed by using XPS. XPS spectra for MWNT: IL (1:5) is displayed in figure 1(b) and the characteristic peaks of expected elements like N (1s), O (1s), F (1s), S (2s), and C (1s) are well resolved. Fingerprint binding energy peak at 402.1 eV represents the N 1s peak in IL modified MWNTs which is absent in pristine MWNT (figure 1(a)). Similarly, the peak at 687.9 eV corresponds to F 1s in the spectra. Detailed convoluted peaks of C 1s and N 1s are shown in figures 1(c), (d).

The interactions between the IL and the MWNTs can be confirmed by FTIR spectroscopy. Figure 2 shows the FTIR of the p-MWNTs and the modified MWNTs. On the addition of IL,

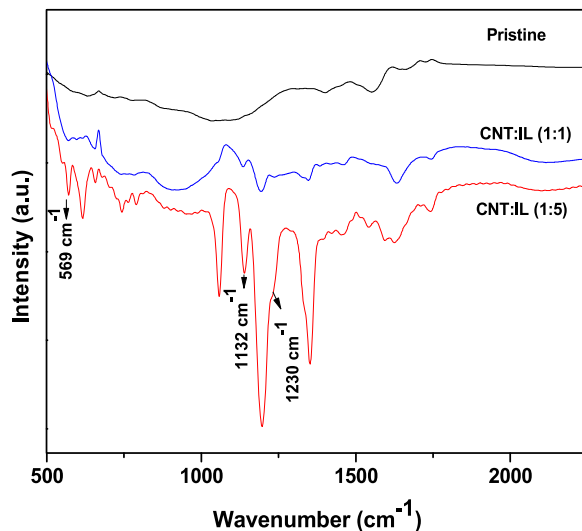
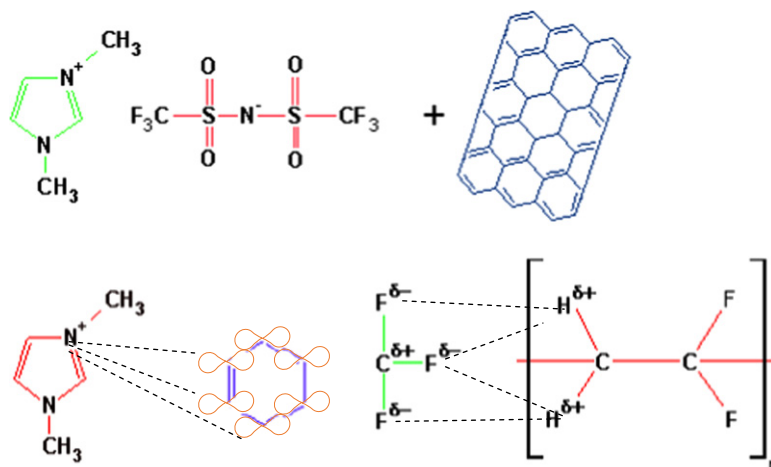


**Figure 2.** FTIR spectra of modified MWNTs.



**Scheme 1.** Schematic illustration showing the possible interactions of ionic liquid with CNTs.

the prominent peaks corresponding to the IL were observed suggesting the presence of IL on the surface of MWNTs and the possible interaction with the MWNTs. The observed peaks at 569, 1132  $\text{cm}^{-1}$  correspond to  $\text{CF}_3$  asymmetrical bending and  $\text{SO}_2$  symmetrical stretching, respectively. The characteristic imidazolium peak at 1165  $\text{cm}^{-1}$  was also obtained which further confirms the presence of the IL. The FTIR peak at 1230  $\text{cm}^{-1}$  corresponds to antisymmetrical stretching of  $\text{CF}_3$  which is also a signature peak of IL. Scheme 1 represents the possible interactions of the IL with the MWNTs, such as cation- $\pi$  interaction between  $\text{EMIM}^+$  of IL with the delocalized  $\pi$ -electron cloud of the MWNTs [23, 24].

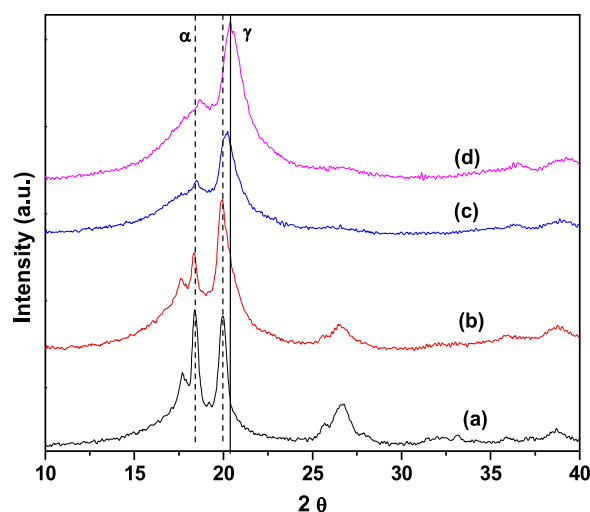


**Figure 3.** XRD patterns of Neat PVDF (a), PVDF with 1 wt% p-CNTs (b), PVDF with 1 wt% IL-MWNTs (1:1) (c) and PVDF with 1 wt% IL-MWNTs (1:5) (d).

### 3.2. IL modified MWNTs induced $\gamma$ crystals in PVDF: assessment through wide angle x-ray diffraction and FTIR

PVDF has five distinct known phases— $\alpha$ ,  $\beta$ ,  $\gamma$ ,  $\delta$  and  $\epsilon$  [25]: the  $\alpha$  phase is obtained directly from the melt and has a conformation of  $(TG^+TG^-)$  with monoclinic crystal structure; the electroactive  $\beta$  phase, which has conformation of  $(TTT)$  with an orthorhombic crystal structure, is quite often desired for designing materials with piezoelectric and energy harvesting materials; the third phase, the  $\gamma$  phase, which is another polar form and has a conformation of  $(TTTG')$ . [21, 26] This phase resembles the  $\beta$  phase and has been investigated in the past for its piezoelectricity and transparency for optical fibers [27].

Figure 3 depicts the XRD peaks of the composite composites. Both PVDF and PVDF with 1 wt% p-CNTs show peaks at  $2\theta$  of 17.6, 18.4 and 26.6° corresponding to the non-polar  $\alpha$ -phase [21]. However, we observe that the PVDF with 1 wt% IL-MWNTs (1:1) and PVDF with 1 wt% IL-MWNTs (1:5) show a very prominent peak of the polar phase  $\gamma$  (110) at the  $2\theta$  value of 20.3° [21] with a broad hump indicating the  $\alpha$ -phase. Thus, addition of the IL modified MWNTs induced the formation of the  $\gamma$  phase in the composites [21].

The changes in the structural information in PVDF composites have further been confirmed using FTIR and are presented in figure 4. In the neat PVDF, characteristic peaks at 614, 764, 974 and 1385  $\text{cm}^{-1}$  correspond to the absorption of the  $\alpha$ -phase [26]. As observed from the spectra, the sharp peaks corresponding to  $\alpha$  crystal phase which were present in PVDF and PVDF with 1 wt% p-CNTs composites are diminished significantly in the PVDF with 1 wt% IL-MWNTs (1:1) and PVDF with 1 wt% IL-MWNTs (1:5) composites. This observation is also in close harmony with those of XRD results where the intensity of the  $\alpha$ -phase is observed to be reduced in the presence of IL modified MWNTs. Interestingly, the peaks at 833 and 1230  $\text{cm}^{-1}$  become more prominent with the addition of IL and correspond to the  $\gamma$ -phase [26] and are thus corroborated with the XRD results. The peak at 872  $\text{cm}^{-1}$  corresponding to the CH-CF-CH stretching [17] in PVDF and PVDF with 1 wt% p-CNTs is observed to shift to a higher frequency of 875  $\text{cm}^{-1}$  for the PVDF with 1 wt% IL-MWNTs (1:1) and PVDF with 1 wt% IL-MWNTs (1:5) composites possibly due to the interaction with IL. From these results

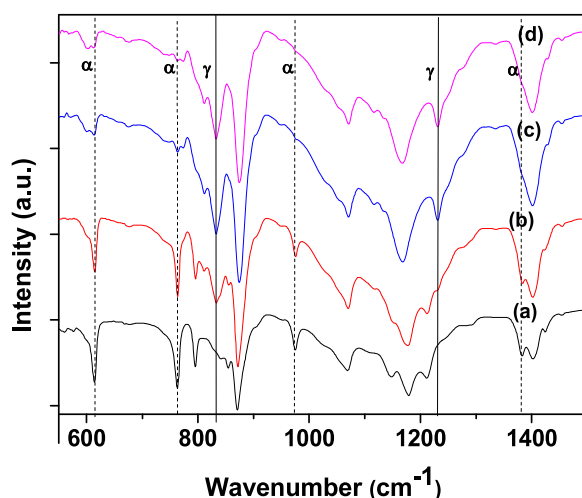


**Figure 4.** FTIR spectra of Neat PVDF (a), PVDF with 1 wt% p-CNTs (b), PVDF with 1 wt% IL-MWNTs (1:1) (c) and PVDF with 1 wt% IL-MWNTs (1:5) (d).

we can conclude that the addition of IL has led to the conversion from  $\alpha$  to  $\gamma$  phase in PVDF. The plausible interaction between PVDF and IL modified MWNTs could be the electrostatic interaction between the anion of the IL and PVDF [21].

Further, we can get an insight on the presence of  $\alpha$ -,  $\beta$ - and  $\gamma$ - phase in the sample by estimating the relative polar fraction ( $F(\beta)$ ) in the sample expressed as,

$$F(\beta) = \frac{X_{\text{polar}}}{X_{\alpha} + X_{\text{polar}}} = \frac{A_{\beta}}{(K_{\beta}/K_{\alpha})A_{\alpha} + A_{\beta}} = \frac{A_{\text{polar}}}{(1.26)A_{\alpha} + A_{\text{polar}}}$$

From the above calculations, the  $F(\text{polar})$  increased with IL modified MWNTs. This polar phase is totally absent in the neat PVDF but increases significantly on incorporation of IL. For example, it increases to 64%, with IL incorporation.

### 3.3. State of dispersion of the pristine and IL modified MWNTs in PVDF: assessing through SEM and melt-rheology

Figures 5(a)–(d) depicts the cryofractured images of neat polymer (5a) and the state of dispersion of 1 wt% MWNTs in PVDF as obtained by SEM. Figure 5(b) shows the agglomeration of the p-CNT in PVDF due to the  $\pi$ - $\pi$  stacking of the MWNTs and would result in poor properties. A good dispersion of fillers in a polymer matrix has been known to show better mechanical properties in terms of strength [8, 26]. Figures 5(c) and (d) show that dispersion of MWNTs has been improved with the addition of IL. The improved interactions of the IL with the MWNTs in the PVDF with 1 wt% IL-MWNTs (1:1) and PVDF with 1 wt% IL-MWNTs (1:5) led to a better dispersion of the MWNTs in the matrix and even much better dispersion in PVDF with 1 wt% IL-MWNTs (1:5). A better dispersion would lead to improved mechanical properties of the composite and will be discussed later. Cation- $\pi$  and/or  $\pi$ - $\pi$  interactions between the imidazolium and MWNTs cause physical gelation of MWNTs and make them swollen, which causes entangled CNTs bundles to exfoliate to form much finer bundles which helps in better dispersion of CNT:IL in PVDF [18, 23, 24].

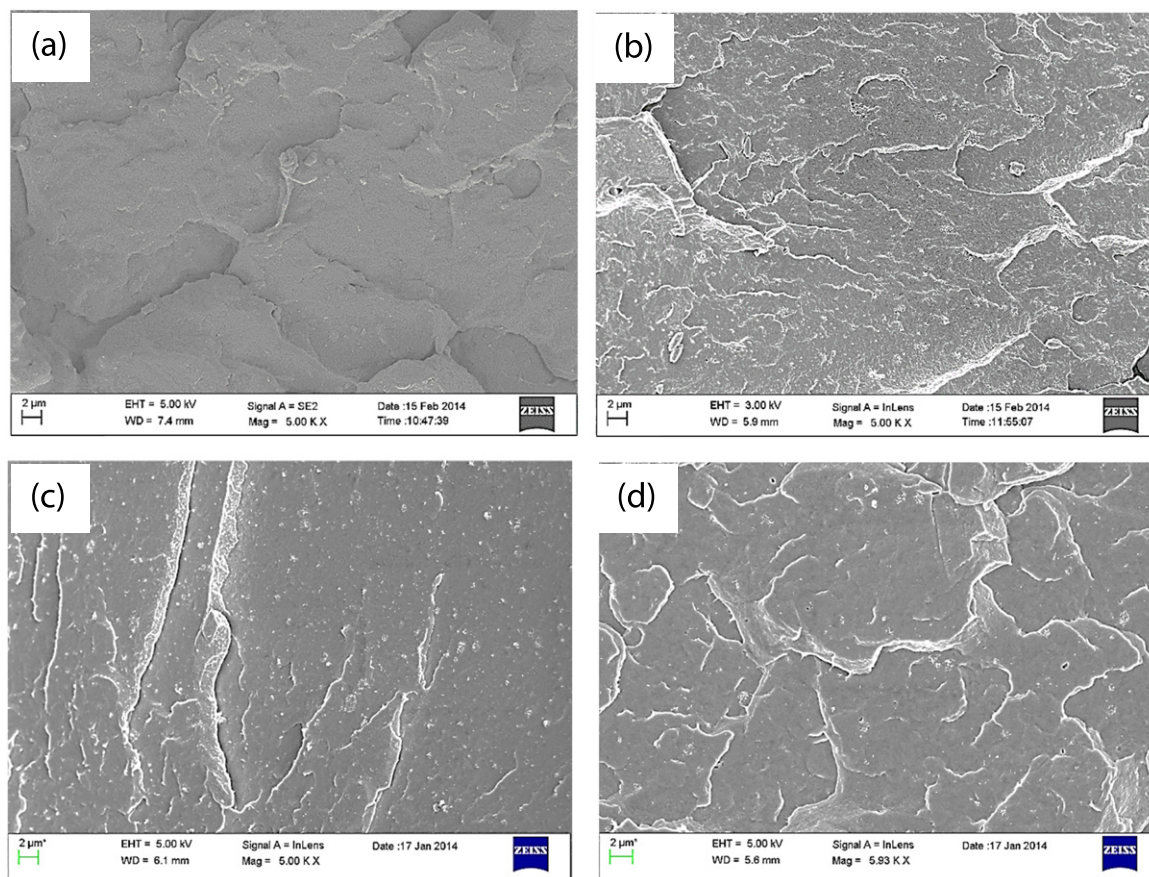


**Figure 5.** SEM images depicting Neat PVDF (a), PVDF with 1 wt% p-CNTs (b), PVDF with 1 wt% IL-MWNTs (1:1) (c) and PVDF with 1 wt% IL-MWNTs (1:5) (d).

Melt-rheological measurements were performed to get insight into the state of dispersion of MWNTs in the composites. Figure 6 depicts the variation of storage modulus with frequency at 200 °C for different composite samples. It is evident from the figure that with the addition of IL modified CNT in PVDF, this causes a decrease in storage modulus over the entire measured frequency range. This suggests the plasticization effect of IL [21]. Plasticization effects of IL in PMMA matrix was reported earlier [28, 29]. Plasticization effect of IL modified MWNTs was further analyzed using DSC.

Figure 7(a) depicts the DSC cooling thermograms of the composite samples cooled from the melt in the first cooling cycle. The  $T_c$  (crystallization temperature) of the PVDF with 1 wt% p-CNTs composite is higher than the neat PVDF. This is possibly due to the heteronucleating effect of CNT [30]. However, with the incorporation of IL modified MWNTs,  $T_c$  further decreases and decreases with an increase in the fraction of IL in the mixture (of MWNT and IL). This suggests that IL is diluting the nucleating effect of MWNTs in the composites and impedes the crystallization of PVDF. In our earlier study, the addition of PMMA in PVDF matrix has resulted in a decrease in  $T_c$  in the blend [5]. Therefore, in PVDF with 1 wt% IL-MWNTs (1:5)  $T_c$  is same as in neat PVDF. A second heating cycle of DSC showing melting behavior of composites is presented in figure 7(b). Interestingly, the addition of 1 wt% IL modified MWNTs in PVDF the  $T_m$  (melting temperature) of the composites has increased.  $T_m$  values for

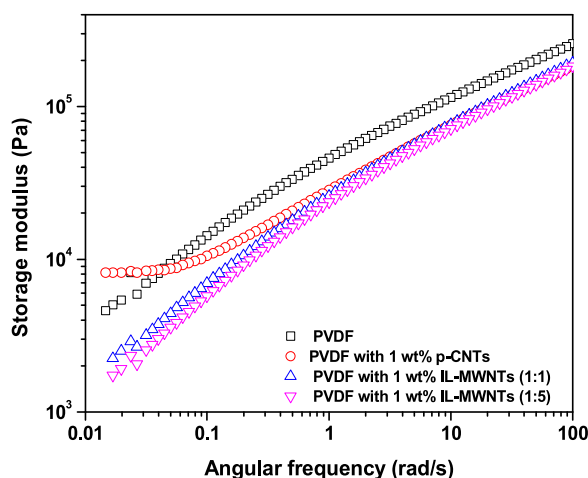


**Figure 6.** Rheology plots of composite samples obtained at 1% strain in the frequency range of (0.01 to 100 rad s<sup>-1</sup>) at 200 °C.

composites are listed in table 2. It has been reported that melting temperature of  $\gamma$  crystals is higher than the  $\alpha$  phase [31, 32]. The presence of double melting as well as abrupt increase in  $T_m$  can be accredited to the presence of polar  $\gamma$ - phase in the composite [21]. Miscibility and plasticization effect of IL in PVDF matrix is further investigated by glass transition temperature ( $T_g$ ) using DSC scans. As reported, the plausible reason of the miscibility between PVDF and IL is due to the specific interaction between imidazolium ions with  $-CF_2$ . Due to this miscibility, glass transition of PVDF decreases with increases in the IL fraction shown in figure 7(c). Thus, a decrease in  $T_g$  with the increase in the IL content can also be attributed to the plasticizer effects of IL in PVDF.

### 3.4. IL induced network formation of MWNTs: effect on electrical conductivity and EMI shielding

The electrical conductivity of the composites was measured and recorded as a function of frequency at 25 °C. Neat PVDF is known to be an insulating polymer with a conductivity value close to  $10^{-13}$  s cm<sup>-1</sup>. Composites with 1 wt% p-CNTs also showed insulating behavior possibly due to agglomeration further leading to the loss of network. Interestingly, on addition of 1 wt% IL modified CNTs (1:1), the conductivity value reached  $10^{-7}$  s cm<sup>-1</sup>. More interestingly, PVDF with 1 wt% IL-MWNTs (1:5) exhibited a lower conductivity. This could be attributed to exfoliations of CNTs in presence of IL thereby impeding the geometrical contact between MWNTs. In fact, the imidazolium ion noncovalently wrapped the CNTs to cause better dispersion of CNT:IL in polymer matrices. Comparatively, the 2 wt% samples showed a distinct improvement in conductivity. They reached an early percolation and thus indicated a good network formation within the matrix. The PVDF with 2 wt% p-CNTs composite also shows better conductivity due to formation of network in the PVDF matrix. The conductivity of PVDF with 2 wt% p-CNTs and PVDF with 2 wt% IL-MWNTs (1:1) jumped to orders of  $10^{-4}$  and  $10^{-3}$  s cm<sup>-1</sup>, respectively. The PVDF with 2 wt% IL-MWNTs (1:5) composites also showed an improvement in conductivity by an order of 3.

The dc conductivity of the composites can be explained using an equation known as the power law:

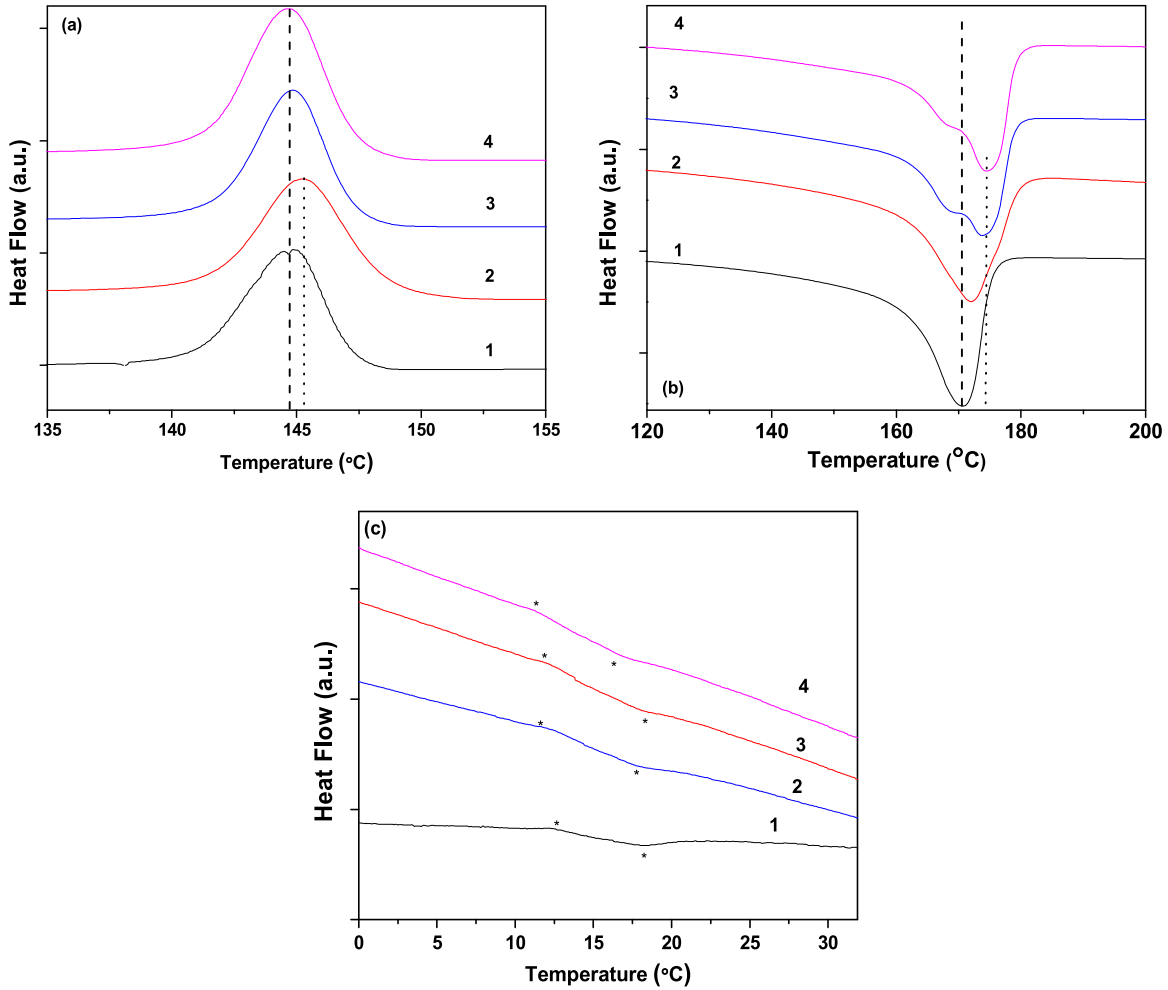


**Figure 7.** DSC scans of composites, representing cooling scans showing crystallization (a), melting scans (b), and glass transition temperature  $T_g$  (c) where (1) is PVDF, (2) PVDF with 1 wt% p-CNTs, (3) PVDF with 1 wt% IL-MWNTs (1:1) (4) and PVDF with 1 wt% IL-MWNTs (1:5).

$$\Sigma_{ac}(\omega) = \sigma_{dc} + A\omega^n$$

Where  $\sigma_{dc}$  is the dc conductivity,  $A$  is a temperature dependent co-efficient,  $\omega$  is the angular frequency and  $n$  is the exponent dependent on both temperature and frequency. The value of  $n$  varies from 0 to 1. The scaling law [33] fits on the conductivity plots revealed a value of 0.65 and 0.7 for PVDF with 2 wt% IL-MWNTs (1:1) and PVDF with 2 wt% p-CNTs, respectively, suggesting nearly a 70–30 resistance capacitance network formation. The mechanism for conductivity can thus be attributed to the tunneling of electrons. Figures 9(a) and (b) show the conductivity of the 1% and 2% composites, respectively.

As mentioned in the introduction, there are two mechanisms of EMI namely reflection and absorption. Possibly in our composite samples, shielding by reflection is more predominant than that by absorption. Reflection is enhanced by connectivity and conductivity [3] and the addition of CNTs has made the composites conducting. Hence, a good dispersed better connected specimen will give rise to a better shield. Since, in CNT based composites, the primary

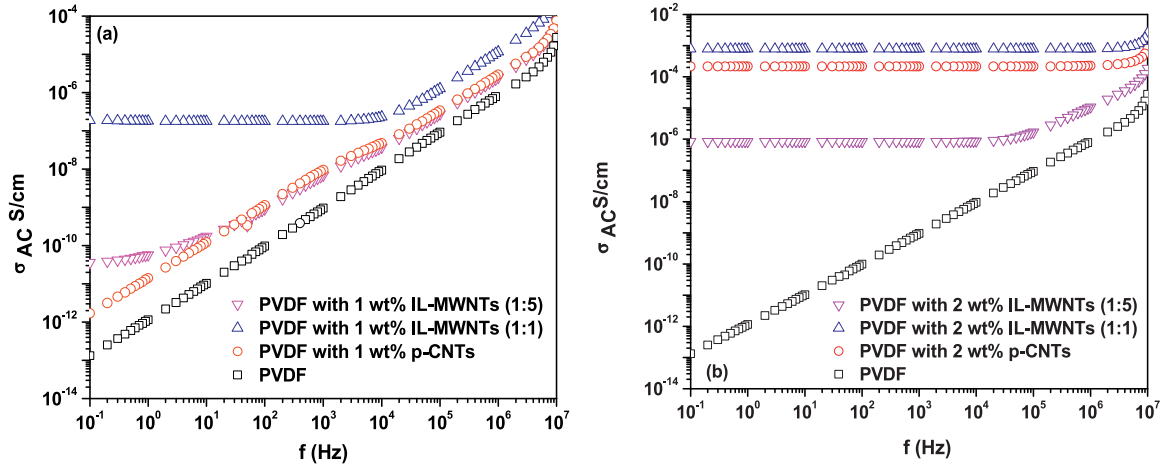


**Figure 8.** Ac conductivity of (a) 1% PVDF with pristine and modified CNTs and (b) 2% PVDF with pristine and modified CNTs.

**Table 2.** Thermal properties of the composites obtained from DSC.

Sample	$T_c$ °C	$T_m$ °C	$T_g$ °C	$X_c$ , %
PVDF	147.3	167.2	15.7	40
PVDF with 1 wt% p-CNTs	148.7	174.7	16.5	33
PVDF with 1 wt% IL-MWNTs (1:1)	147.4	173	14.6	37
PVDF with 1 wt% IL-MWNTs (1:5)	147.3	174.8	14.4	35

mechanism for shielding is reflection, composites which possess a greater conductivity will lead to better shielding.

To calculate reflection, absorption and total SE, there are standard formulae available in the literature [34]:

$$SE_R (\text{shielding by reflection}) = 10 \log_{10} (1/(1 - (S_{11})^2))$$

$$SE_A (\text{shielding by absorption}) = 10 \log_{10} ((1 - [S_{11}]^2)/[S_{12}]^2)$$

$$SE_T (\text{total shield effectiveness}) = SE_R + SE_A = 10 \log (1/[S_{12}]^2)$$

where  $S_{11}$  and  $S_{12}$  are known as scattering parameters.

The SE of the neat PVDF is known to be close to zero as it is insulating and is transparent to the radiation. PVDF with 1 wt% p-CNTs and PVDF with 1 wt% IL-MWNTs (1:1) show almost the same EMI values of close to 7 dB but the conductivity of the two composites is very different. This can be explained as connectivity is not always necessary for SE though it is enhanced by it [3]. Hence, as IL ensures a very good dispersion and thus a loss in connectivity, we see that the SE of PVDF with 1 wt% IL-MWNTs (1:5) and PVDF with 2 wt% IL-MWNTs (1:5) are close to 5 dB, which is lower than other composites. In PVDF with 1 wt% IL-MWNTs (1:5) and PVDF with 2 wt% IL-MWNTs (1:5), the amount of MWNTs present is also less compared to the 1:1 composites. This could also be a reason for poor shield effectiveness. Following conductivity, the SE of PVDF with 2 wt% IL-MWNTs (1:1) is higher and reach values of 18 dB in comparison to PVDF with 2 wt% p-CNTs (15 dB), which is sufficient for

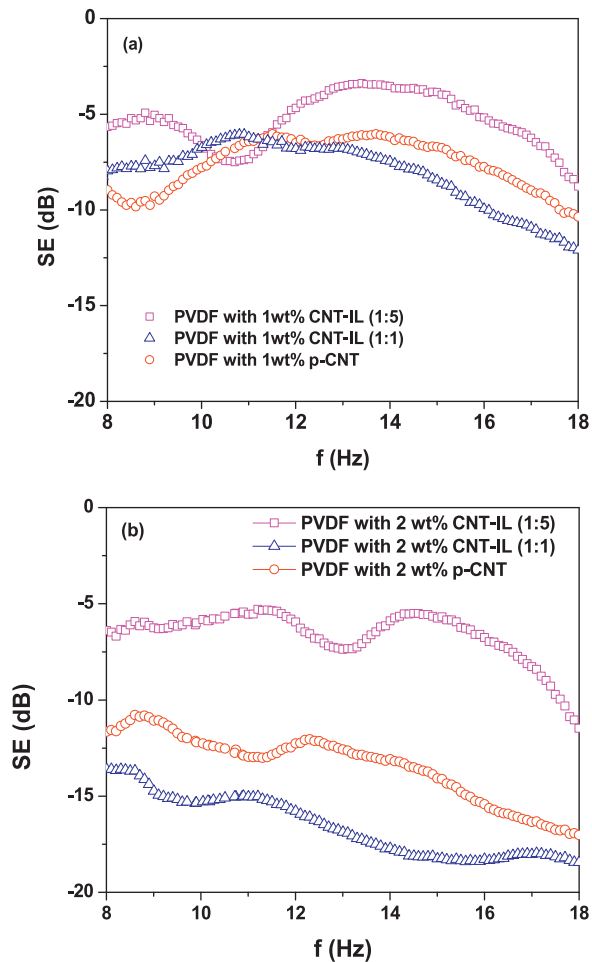


**Figure 9.** SE as a function of frequency of (a) 1 wt% PVDF composites and (b) 2 wt% PVDF composites.

some commercial applications. Figures 9(a) and (b) show the SE of 1% and 2% composites, respectively.

### 3.5. Mechanical properties and flexibility of the film: tensile testing

PVDF inherently possesses moderate mechanical properties. On addition of MWNTs, the structural property can further be improved, provided the dispersion is good. The load carrying capacity of our composites was measured as a function of their elongation. We observed that the composites with p-MWNTs are extremely brittle, in striking contrast to IL modified MWNTs composites. The PVDF with 1 wt% IL-MWNTs (1:1) and PVDF with 1 wt% IL-MWNTs (1:5) show a large improvement in terms of strength and ductility when compared to neat PVDF and PVDF with 1 wt% p-CNTs. In 2% composites, there is a slight loss in ductility of the PVDF with 2 wt% IL-MWNTs (1:1) and PVDF with 2 wt% IL-MWNTs (1:5) composites. PVDF with 2 wt% IL-MWNTs (1:1) is still better than the neat and pristine composites in terms of ductility and shows only a marginal loss in elongational properties, in striking contrast to p-MWNTs. Figures 10(a)–(h) depict the mechanical properties of the composites, and values of tensile strength and Young's modulus are listed in table 3.

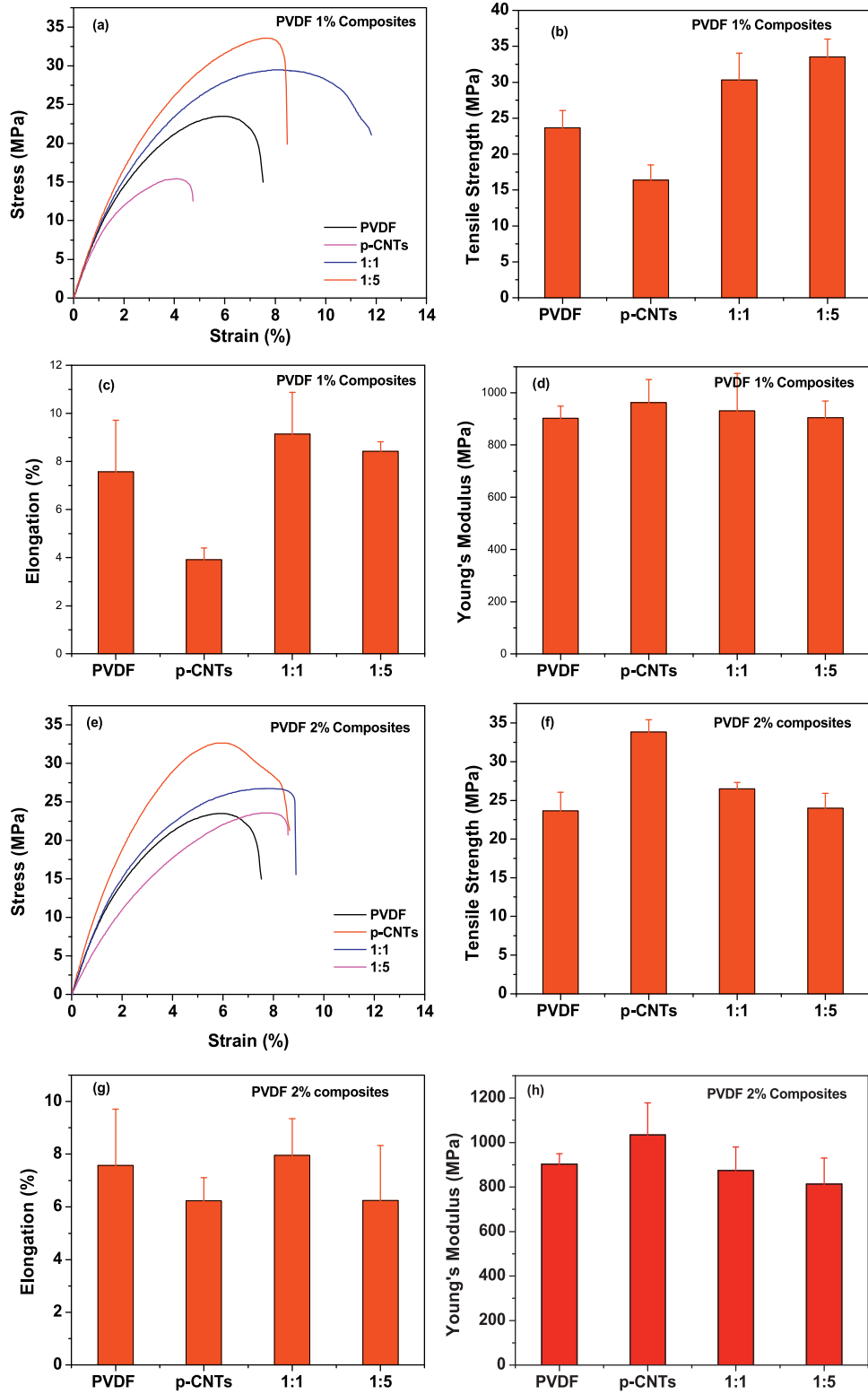


**Figure 10.** Mechanical properties of 1% PVDF composites (a)-(d) and 2% composites (e)-(h).

**Table 3.** Mechanical properties values obtained by the Micro UTM.

Sample Designation	Tensile Strength (MPa)	Elongation at break (%)	Young's Modulus (MPa)
PVDF	26.6	7.6	902
PVDF with 1 wt% p-CNTs	16.4	3.9	962
PVDF with 1 wt% IL-MWNTs (1:1)	30.3	9.1	930
PVDF with 1 wt% IL-MWNTs (1:5)	33.5	8.4	904
PVDF with 2 wt% p-CNTs	33.8	6.2	1034
PVDF with 2 wt% IL-MWNTs (1:1)	24.5	7.9	874
PVDF with 2 wt% IL-MWNTs (1:5)	24.0	6.2	813

#### 4. Conclusions

PVDF Nano-composites of varying percentages of modified CNTs and varying ratios (1:1 and 1:5) of IL were prepared by melt mixing. These composites were characterized for interaction with the ionic liquid, dispersion, crystalline morphology, conductivity, EMI shielding and mechanical properties.

We observed an electrostatic interaction and cation- $\pi$  interaction between the CNTs and IL. By conducting FTIR and XRD we concluded a non-covalent interaction of PVDF with the modified CNTs as well as increment of  $\gamma$ -phase with the addition of the modified CNTs and this was supported by DSC scans. Double melting peaks were observed for composites samples. Plasticization effects of IL in PVDF matrix were confirmed by using DSC as well as with rheology scans. SEM images proved a good dispersion of IL in PVDF matrix and dispersion become better with the increase in the IL fraction in the composites. The conductivity of the composites was also seen to increase significantly with the addition of 1:1 modified CNTs but not so much with the addition of 1:5 modified CNTs. Hence by increasing the concentration of the IL, the conductive properties were seen being hampered because of non-covalent coating of IL over CNTs which disrupts the  $\pi$ -cloud over CNTs. The SE of the specimens also followed the trend of conductivity and high values of 20 Db were obtained in the Ku band by PVDF with 2 wt% IL-MWNTs (1:1) composites. The primary mechanism of shielding was observed to be reflection. The mechanical properties of the composites were also seen to increase with the addition of the 1:1 modified CNTs. Hence, we were successful in making a flexible and easy to process EMI shielding material for commercial applications.

#### Acknowledgements

The authors gratefully thank Arkema Inc. for kindly providing PVDF. We would also like to acknowledge MNCF, Cense, IISc for providing the characterization facilities.

## References

- [1] Hossmann K A and Hermann D 2003 Effects of electromagnetic radiation of mobile phones on the central nervous system *Bioelectromagnetics* **24** 49–62
- [2] Zhu W *et al* 2011 Electromagnetic and microwave-absorbing properties of magnetic nickel ferrite nanocrystals *Nanoscale* **3** 2862–4
- [3] Chung D 2001 Electromagnetic interference shielding effectiveness of carbon materials *Carbon* **39** 279–85
- [4] Joseph N *et al* 2013 Effect of silver incorporation into PVDF-barium titanate composites for EMI shielding applications *Mater. Res. Bull.* **48** 1681–7
- [5] Sharma M, Madras G and Bose S 2014 Size dependent structural relaxations and dielectric properties induced by surface functionalized MWNTs in poly (vinylidene fluoride)/poly (methyl methacrylate) blends *Phys. Chem. Chem. Phys.* **16** 2693–704
- [6] Bergman J Jr, McFee J and Crane G 2003 Pyroelectricity and optical second harmonic generation in polyvinylidene fluoride films *Appl. Phys. Lett.* **18** 203–5
- [7] Salimi A and Yousefi A 2003 Analysis method: FTIR studies of  $\beta$ -phase crystal formation in stretched PVDF films *Polym. Test* **22** 699–704
- [8] Li Y and Shimizu H 2008 Conductive PVDF/PA6/CNTs nanocomposites fabricated by dual formation of cocontinuous and nanodispersion structures *Macromolecules* **41** 5339–44
- [9] Lee B *et al* 2002 Influence of aspect ratio and skin effect on EMI shielding of coating materials fabricated with carbon nanofiber/PVDF *J. Mater. Sci.* **37** 1839–43
- [10] Eswaraiyah V, Sankaranarayanan V and Ramaprabhu S 2011 Inorganic nanotubes reinforced polyvinylidene fluoride composites as low-cost electromagnetic interference shielding materials *Nanoscale Res. Lett.* **6** 1–11
- [11] Kim W-S *et al* 2002 Electrical properties of PVDF/PVP composite filled with carbon nanotubes prepared by floating catalyst method *Macromol. Res.* **10** 253–8
- [12] Coleman J N, Khan U and Gun'ko Y K 2006 Mechanical reinforcement of polymers using carbon nanotubes *Adv. Mater.* **18** 689–706
- [13] Postma H W C, Teepen T, Yao Z, Grifoni M and Dekker C 2001 Carbon nanotube single-electron transistors at room temperature *Science* **293** 76–9
- [14] Pop E, Mann D, Wang Q, Goodson K and Dai H 2006 Thermal conductance of an individual single-wall carbon nanotube above room temperature *Nano Lett.* **6** 96–100
- [15] Saini P, Choudhary V, Singh B, Mathur R and Dhawan S 2009 Polyaniline–MWCNT nanocomposites for microwave absorption and EMI shielding *Mater. Chem. Phys.* **113** 919–26
- [16] Thomassin J-M *et al* 2013 Polymer/carbon based composites as electromagnetic interference (EMI) shielding materials *Mater. Sci. Eng. R* **74** 211–32
- [17] Mandal A and Nandi A K 2013 Ionic liquid integrated multiwalled carbon nanotube in a poly (vinylidene fluoride) matrix: formation of a piezoelectric  $\beta$ -polymorph with significant reinforcement and conductivity improvement *ACS Appl. Mater. Interfaces* **5** 747–60
- [18] Xing C *et al* 2012 Impact of ionic liquid-modified multiwalled carbon nanotubes on the crystallization behavior of poly (vinylidene fluoride) *J. Phys. Chem. B* **116** 8312–20
- [19] Ye Y-S, Rick J and Hwang B-J 2013 Ionic liquid polymer electrolytes *J. Mater. Chem. A* **1** 2719–43
- [20] Carrión F, Espejo C, Sanes J and Bermúdez M 2010 Single-walled carbon nanotubes modified by ionic liquid as antiwear additives of thermoplastics *Compos. Sci. Technol.* **70** 2160–7
- [21] Xing C, Zhao M, Zhao L, You J, Cao X and Li Y 2013 Ionic liquid modified poly(vinylidene fluoride): crystalline structures, miscibility, and physical properties. *Polym. Chem.* **4** 5726–34
- [22] Li N *et al* 2006 Electromagnetic interference (EMI) shielding of single-walled carbon nanotube epoxy composites *Nano Lett.* **6** 1141–5
- [23] Fukushima T *et al* 2003 Molecular ordering of organic molten salts triggered by single-walled carbon nanotubes *Science* **300** 2072–4

- [24] Wang J, Chu H and Li Y 2008 Why single-walled carbon nanotubes can be dispersed in imidazolium-based ionic liquids *ACS Nano* **2** 2540–6
- [25] Mohammadi B, Yousefi A A and Bellah S M 2007 Effect of tensile strain rate and elongation on crystalline structure and piezoelectric properties of PVDF thin films *Polym. Test* **26** 42–50
- [26] Liu L and Grunlan J C 2007 Clay assisted dispersion of carbon nanotubes in conductive epoxy nanocomposites *Adv. Funct. Mater.* **17** 2343–8
- [27] Lopes A, Costa C, Tavares C, Neves I and Lanceros-Mendez S 2011 Nucleation of the electroactive  $\gamma$  phase and enhancement of the optical transparency in low filler content poly (vinylidene)/clay nanocomposites *J. Phys. Chem. C* **115** 18076–82
- [28] Scott M P *et al* 2002 Application of ionic liquids as plasticizers for poly (methyl methacrylate) *Chem. Commun.* 1370–1
- [29] Lunstroot K *et al* 2010 Ionic liquid as plasticizer for europium (III)-doped luminescent poly (methyl methacrylate) films *Phys. Chem. Chem. Phys.* **12** 1879–85
- [30] Sharma M, Sharma K and Bose S 2013 Segmental relaxations and crystallization-induced phase separation in PVDF/PMMA blends in the presence of surface-functionalized multiwall carbon nanotubes *J. Phys. Chem. B* **117** 8589–602
- [31] Ince-Gunduz B S *et al* 2010 Impact of nanosilicates on poly(vinylidene fluoride) crystal polymorphism: part 1. melt-crystallization at high supercooling. *Polymer* **51** 1485–93
- [32] Morra B S and Stein R S 1982 Melting studies of poly(vinylidene fluoride) and its blends with poly(methyl methacrylate) *J. Polym. Sci. Polymer Phys. Ed.* **20** 2243–59
- [33] Mural P K S, Madras G and Bose S 2014 Positive temperature coefficient and structural relaxations in selectively localized MWNTs in PE/PEO blends *RSC Adv.* **4** 4943–54
- [34] Al-Saleh M H, Saadeh W H and Sundararaj U 2013 EMI shielding effectiveness of carbon based nanostructured polymeric materials: a comparative study *Carbon* **60** 146–56